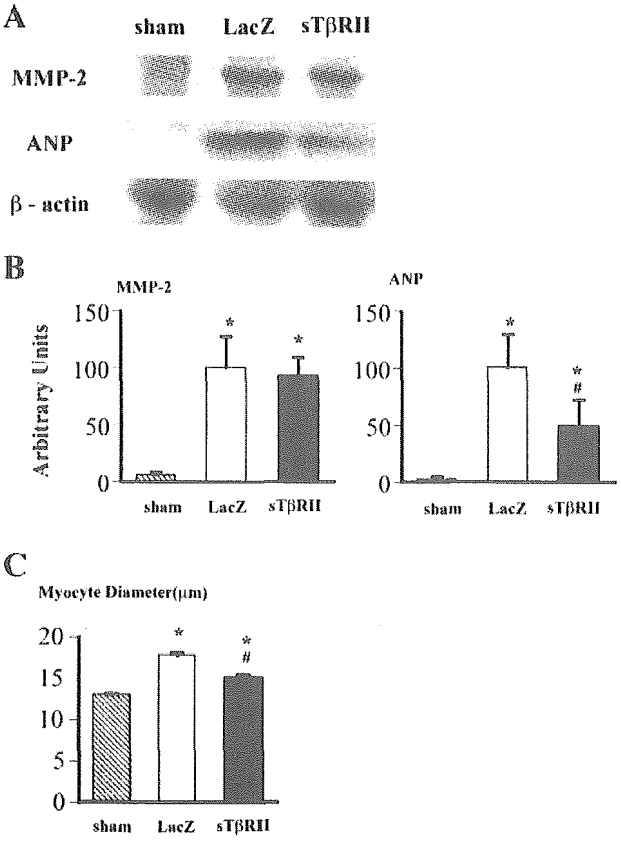

Figure 5. A, Western blotting for MMP-2 and ANP of sham-operated heart and hearts with 4-week-old MI. B, Densitometry of MMP-2 (left) and ANP (right). C, Cardiomyocyte size in sham-operated control hearts and hearts with 4-week-old MI. *$P<0.05$, significant difference compared with sham; #$P<0.05$, significant difference compared with the LacZ-treated MI group.

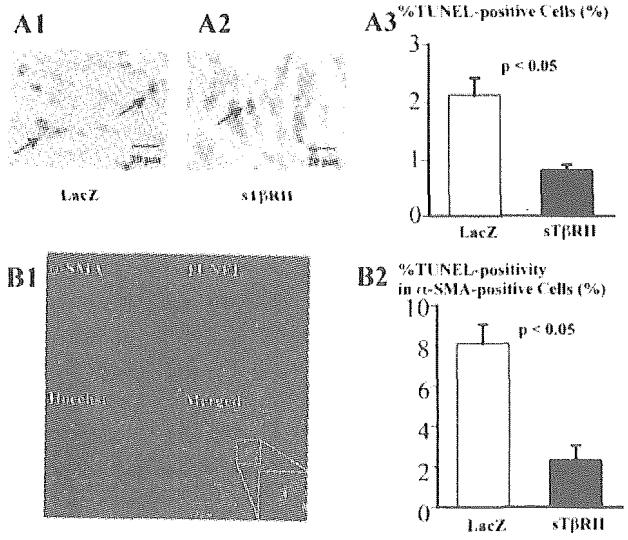

Figure 6. Apoptosis within infarcted tissue 10 days after MI. A, TUNEL-stained preparations from LacZ-treated (A1) and sTβRII-treated (A2) mice. A3, Percentage of TUNEL-positive nonmyocytes within the infarcted area. Arrows indicate positive cells. B, Infarcted tissue obtained from LacZ-treated mice (B1) was double stained with TUNEL and α-SMA immunohistochemistry and observed under a confocal microscope. B2, Percentage of TUNEL-positive cells among the α-SMA–positive cells.

Ten Days After MI

By 10 days after MI, the infarcted areas were composed of granulation tissue, and TUNEL assays indicated that apoptosis was ongoing in both the LacZ- and sTβRII-treated groups. However, the incidence of TUNEL-positive cells was significantly smaller in the sTβRII-treated than in the LacZ-treated group (Figure 6A1 to 6A3). Moreover, double-immunofluorescence assays (TUNEL followed by anti–Flk-1 or anti–SMA antibody) revealed that within the sTβRII-treated group, the incidence of apoptosis was reduced among myofibroblasts/smooth muscle cells (Figure 6B1 and 6B2) but not among endothelial cells (LacZ, 3.5±0.5% versus sTβRII, 3.5±0.2%; P=NS), which suggests that sTβRII may specifically inhibit apoptosis among myofibroblasts. TUNEL-positive cardiomyocytes were extremely rare (<0.01%) in both groups.

Effect of sTβRII on Fas-Induced Apoptosis In Vitro (Protocol 2)

Myofibroblasts obtained from the infarcted areas of mouse hearts 10 days after MI were cultured in medium containing 5% serum collected from LacZ- or sTβRII-treated mice. When the cells were then subjected to Fas-induced apoptosis[16] for 24 hours, the incidence of TUNEL-positive myofibroblasts was significantly lower among cells cultured with sTβRII-containing serum (16±2.9%) than among those cultured with normal serum (43±5.2%; $P<0.05$) (Figure 7). However, such an apoptosis-inhibitory effect by sTβRII-containing serum was completely canceled by an addition of TGF-β1 at the concentration of 1 μg/mL (Figure 7). These findings suggest that sTβRII exerts a direct antiapoptotic effect on cardiac myofibroblasts.

Effect of Anti–TGF-β Treatment at Chronic Stage (Protocol 3)

Using protocol 3, we determined the extent to which inhibiting apoptosis among granulation tissue cells is responsible for the beneficial effects on post-MI heart failure. For this purpose, the sTβRII gene therapy was started at a more chronic stage of MI, after the granulation tissue had already been replaced with scar tissue. The sTβRII (n=14) or LacZ (n=11) gene was delivered to mice 4 weeks after MI, and the mice were examined after an additional 4 weeks (8 weeks after MI). Accessibility of sTβRII into scar tissue was confirmed by Western blotting (Figure 1B). One of 14 sTβRII-treated mice and none of the 11 LacZ-treated mice died during the additional 4-week follow-up (P=NS). This time we found no difference in ventricular geometry or function between the sTβRII-treated and LacZ-treated groups (Table), clearly indicating that the preventive effect of sTβRII gene therapy on heart failure is attributable to its action on granulation tissue during the subacute stage of MI.

Discussion

The present study revealed that postinfarction sTβRII gene therapy, begun at the subacute stage of MI, alleviated adverse remodeling and improved function of the LV during the chronic stage. In addition, we provide novel insights into the

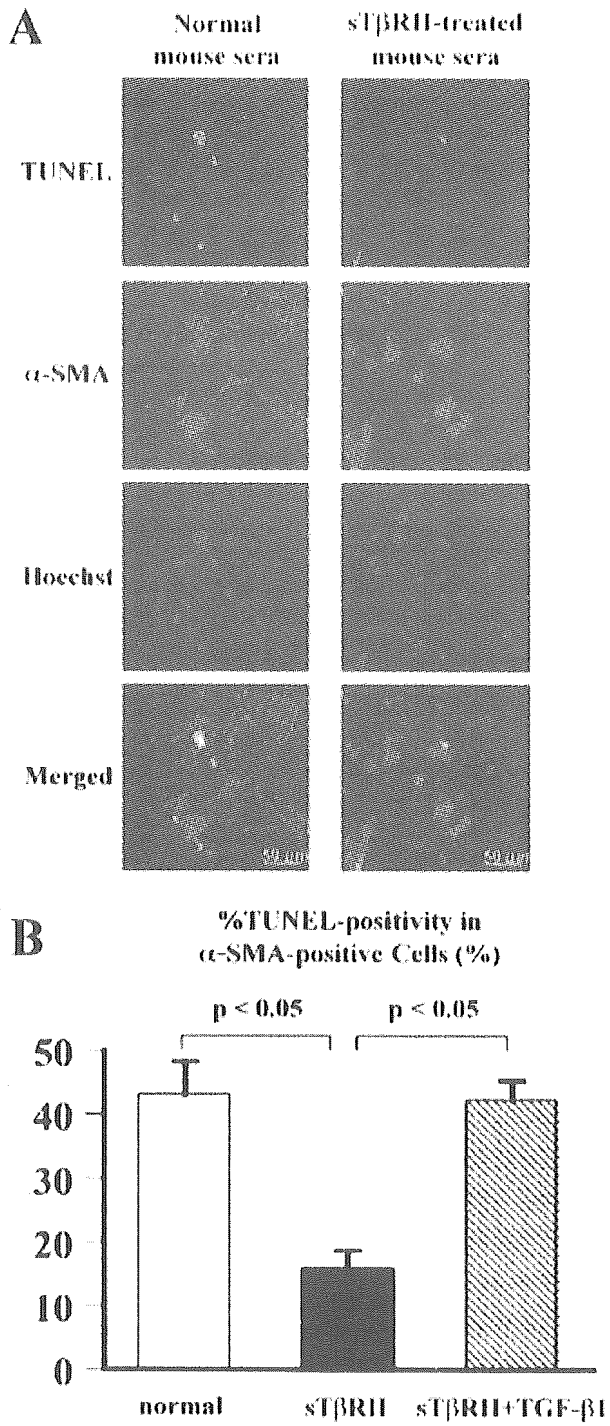

Figure 7. Effect of sTβRII-containing sera on Fas-induced apoptosis among cultured nonmyocytes obtained from the infarcted tissue of hearts 10 days after MI (protocol 2). Confocal micrographs (A) show TUNEL-positive/α-SMA–positive cultured cells. B, Percentage of apoptotic myofibroblasts.

mechanism of the beneficial effect of the TGF-β signal inhibition.

Mechanisms of Beneficial Effects of sTβRII on Postinfarction Heart Failure

The mechanisms responsible for the beneficial effects of inhibiting TGF-β signaling on post-MI heart failure appear somewhat complicated, probably reflecting the multiple biological effects of TGF-β. TGF-β signaling acts as a strong inducer of extracellular matrix and as an immunomodulator of chemotaxis by fibroblasts and inflammatory cells.[18–20] In the infarcted heart, TGF-β expression is regulated by locally generated angiotensin II via angiotensin II type 1 receptor binding, and angiotensin-converting enzyme inhibitors and angiotensin II type 1 receptor blockade attenuated postinfarction ventricular remodeling equally.[11,12] However, the manner in which direct inhibition of TGF-β signaling in the infarcted heart affects the postinfarction process has not been well elucidated . In the present study inhibition of TGF-β signaling by exogenous sTβRII significantly reduced cardiac fibrosis, confirming the fibrogenetic effect of TGF-β on post-MI hearts. Because myocardial fibrosis contributes to both systolic and diastolic dysfunction in the heart,[6,7] reducing it by inhibiting TGF-β signaling is one way in which to mitigate LV remodeling and heart failure. MMP-2 activity seemed to be not significantly associated with sTβRII-induced antifibrosis in the present experimental setting.

Perhaps the most notable finding of the present study is the effect of anti–TGF-β therapy on infarct geometry, ie, the shortening of the infarcted segment and the thickening of the infarcted wall, without a change in absolute infarcted area. Contraction of the infarcted tissue likely contributes to suppression of LV dilatation. Because wall stress is proportional to the cavity diameter and inversely proportional to the wall thickness (Laplace's law)[21] and because wall stress and adverse LV remodeling (dilatation) have a vicious relationship, accelerating one another, it is easy to surmise that such an alteration in the geometry of the infarct would markedly improve the hemodynamic state of the heart.

Ventricular Geometry, Function, and Histology 8 Weeks After MI Among Mice Transfected With the Indicated Gene 4 Weeks After MI (Protocol 3)

	LacZ (n=11)	sTβRII (n=13)	P
LVED diameter, mm	6.0±0.1	6.3±0.2	0.11
% Fractional shortening	16.7±0.6	16.1±0.6	0.53
Heart rate, bpm	502±21	544±20	0.16
LVSP, mm Hg	85±3	80±3	0.21
LVEDP, mm Hg	9±1	9±1	0.84
+dP/dt, mm Hg/s	3847±101	3608±150	0.22
−dP/dt, mm Hg/s	−3642±166	−3337±144	0.18
MI area, $\times 10^3$ μm^2	2.1±0.2	2.4±0.3	0.53
% MI area	21.5±3.2	24.2±3.0	0.57
MI segmental length, $\times 10^3$ μm	6.1±0.9	6.4±0.7	0.78
MI wall thickness, $\times 10^2$ μm	2.4±0.4	2.0±0.2	0.43
% Fibrosis in non-MI area	17.7±1.8	18.1±1.9	0.88
% Fibrosis in MI area	50.6±3.6	51.5±3.9	0.56
Cell population in MI area, cells/10^5 μm^2	149±6	144±5	0.56
Area of α-SMA–positive cells, %	1.9±0.9	2.0±0.2	0.75

LVED indicates LV end-diastolic; LVSP, LV peak systolic pressure; and LVEDP, LV end-diastolic pressure.

Inhibition of TGF-β signaling also qualitatively altered the infarct tissue. We found an increased abundance of α-SMA–positive cells (myofibroblasts and smooth muscle cells) in the extravascular area of infarcts in sTβRII-treated hearts. Those cells are well known to play an important role in wound contraction during the healing process,[22] and to then disappear via apoptosis.[23,24] Recently, we reported that blockade of myofibroblast apoptosis by the treatment with pan-caspase inhibitor or with soluble Fas, a competitive inhibitor of Fas, attenuates postinfarction ventricular remodeling and heart failure.[25,26] We speculate that the preserved myofibroblasts may contribute structurally to the thickening of the infarct scar. In addition, although the property of contractile function of these myofibroblasts has not been elucidated, it is conceivable that contractile myofibroblasts that are running parallel with the infarct circumference may shrink the infarct into coronal directions and increase the infarct thickness.

It is thus notable that sTβRII had a direct inhibitory effect on apoptosis among myofibroblasts in granulation tissue, both in vivo and in vitro. This is consistent with the report by Hagimoto et al,[27] who showed that TGF-β1 sensitizes pulmonary epithelial cells to Fas-induced apoptosis. Conversely, TGF-β is known to promote transdifferentiation of fibroblasts into myofibroblasts,[28] ie, inhibition of TGF-β signaling possibly results in reduction of myofibroblast population. Inhibition of TGF-β signaling thus appears to have reciprocal effects on myofibroblast population: its reduction through interfering with transdifferentiation from fibroblasts and its augmentation through blocking apoptotic death. In the present experimental setting, the gene product peaked during the granulation tissue phase (1-week-old infarct) when myofibroblasts were already abundant but their apoptosis was ongoing. In the 4-week-old infarct tissue, however, naturally occurring apoptosis was already complete in the control MI hearts. These findings may explain our data that the population of α-SMA–positive cells was balanced to gain in the post-MI scar tissue of the TGF-β signal–inhibited hearts. Taken together, these findings suggest that myofibroblasts escaping apoptosis may survive even during the chronic stage of MI, accumulate, form bundles, and contribute to infarct contraction. In addition, this mechanism appears critical for functional improvement, as transfection of the sTβRII gene was ineffective if started during the chronic stage of MI, when most α-SMA–positive cells have already disappeared (see protocol 3 above).

Because in the present study sTβRII gene therapy was started on the third day after MI, it is unlikely that it influenced cardiomyocyte apoptosis during the acute stage. It is also unlikely that this therapy affected cardiomyocyte survival by inhibiting apoptosis at the subacute or chronic stages. This is because, in contrast to an earlier report,[4] we found that apoptosis was negligible among cardiomyocytes at any stage of MI.

Time Window Within Which to Inhibit TGF-β Signaling

TGF-β signaling is believed to have cardioprotective effect during ischemia/reperfusion, perhaps as a result of inhibition of tumor necrosis factor-α release, improvement of endothelium-dependent relaxation, prevention of reactive oxygen species generation, and/or inhibition of upregulation of matrix metalloproteinase-1.[29,30] For these reasons, inhibition of TGF-β signaling during the acute stage of MI is considered harmful. In addition, our data indicate that late inhibition of TGF-β signaling (during the scar phase of MI) is without effect. It thus appears that there is a therapeutic time window that is critical for inhibition of TGF-β signaling to elicit the beneficial effects on post-MI heart failure.

Limitations and Clinical Implications

There is considerable evidence indicating that the TGF-β signal exerts a protective effect against atherosclerosis in mouse models by preventing lipid lesion formation.[31–33] This potential limitation might have to be taken into account in application of the anti–TGF-β strategy.

Rapid recanalization of the occluded coronary artery is presently the best clinical approach to the treatment of acute MI; if performed in time, it enables salvage of the ischemic myocardial cells. Unfortunately, most patients miss the chance for coronary reperfusion therapy because to be effective it must be performed within a few hours after the onset of infarction.[34] The present findings suggest that this novel therapeutic strategy may mitigate the chronic progressive heart failure seen in patients after large MIs. When initiated during the subacute stage, inhibition of TGF-β signaling may benefit patients who missed the chance for coronary reperfusion.

Acknowledgments

We thank Akiko Tsujimoto and Hatsue Ohshika for technical assistance.

References

1. Pfeffer MA, Braunwald E. Ventricular remodeling after myocardial infarction: experimental observations and clinical implications. *Circulation.* 1990;81:1161–1172.
2. Hosenpud JD, Bennett LE, Keck BM, Boucek MM, Novick RJ. The Registry of the International Society for Heart and Lung Transplantation: seventeenth official report: 2000. *J Heart Lung Transplant.* 2000;19:909–931.
3. Pfeffer JM, Pfeffer MA, Fletcher PJ, Braunwald E. Progressive ventricular remodeling in rat with myocardial infarction. *Am J Physiol.* 1991;260:H1406–H1414.
4. Cheng W, Kajstura J, Nitahara JA, Li B, Reiss K, Liu Y, Clark WA, Krajewski S, Reed JC, Olivetti G, Anversa P. Programmed myocyte cell death affects the viable myocardium after infarction in rats. *Exp Cell Res.* 1996;226:316–327.
5. Weisman HF, Bush DE, Mannisi JA, Weisfeldt ML, Healy B. Cellular mechanisms of myocardial infarct expansion. *Circulation.* 1988;78:186–201.
6. Burlew BS, Weber KT. Connective tissue and the heart: functional significance and regulatory mechanisms. *Cardiol Clin.* 2000;18:435–442.
7. Jalil JE, Doering CW, Janicki JS, Pick R, Shroff SG, Weber KT. Fibrillar collagen and myocardial stiffness in the intact hypertrophied rat left ventricle. *Circ Res.* 1989;64:1041–1050.
8. Lijnen PJ, Petrov VV, Fagard RH. Induction of cardiac fibrosis by transforming growth factor-beta1. *Mol Genet Metab.* 2000;71:418–435.
9. Hao J, Ju H, Zhao S, Junaid A, Scammell-La Fleur T, Dixon IM. Elevation of expression of Smad2, 3, and 4, decorin and TGF-beta in the chronic phase of myocardial infarct scar healing. *J Mol Cell Cardiol.* 1999;31:667–678.
10. Deten A, Holzl A, Leicht M, Barth W, Zimmer HG. Changes in extracellular matrix and in transforming growth factor beta isoforms after coronary artery ligation in rats. *J Mol Cell Cardiol.* 2001;33:1191–1207.
11. Schieffer B, Wirger A, Meybrunn M, Seitz S, Holtz J, Riede UN, Drexler H. Comparative effects of chronic angiotensin-converting enzyme inhi-

bition and angiotensin II type 1 receptor blockade on cardiac remodeling after myocardial infarction in the rat. *Circulation.* 1994;89:2273–2282.
12. Yu CM, Tipoe GL, Wing-Hon Lai K, Lau CP. Effects of combination of angiotensin-converting enzyme inhibitor and angiotensin receptor antagonist on inflammatory cellular infiltration and myocardial interstitial fibrosis after acute myocardial infarction. *J Am Coll Cardiol.* 2001;38:1207–1215.
13. Isaka Y, Akagi Y, Ando Y, Tsujie M, Sudo T, Ohno N, Border WA, Noble NA, Kaneda Y, Hori M, Imai E. Gene therapy by transforming growth factor-beta receptor-IgG Fc chimera suppressed extracellular matrix accumulation in experimental glomerulonephritis. *Kidney Int.* 1999;55:465–475.
14. Li Y, Takemura G, Kosai K, Yuge K, Nagano S, Esaki M, Goto K, Takahashi T, Hayakawa K, Koda M, Kawase Y, Maruyama R, Okada H, Minatoguchi S, Mizuguchi H, Fujiwara T, Fujiwara H. Postinfarction treatment with an adenoviral vector expressing hepatocyte growth factor relieves chronic left ventricular remodeling and dysfunction in mice. *Circulation.* 2003;107:2499–2506.
15. Chen SH, Chen XH, Wang Y, Kosai K, Finegold MJ, Rich SS, Woo SL. Combination gene therapy for liver metastasis of colon carcinoma in vivo. *Proc Natl Acad Sci U S A.* 1995;92:2577–2581.
16. Katwa LC, Campbell SE, Tyagi SC, Lee SJ, Cicila GT, Weber KT. Cultured myofibroblasts generate angiotensin peptides de novo. *J Mol Cell Cardiol.* 1997;29:1375–1386.
17. Ni R, Tomita Y, Matsuda K, Ichihara A, Ishimura K, Ogasawara J, Nagata S. Fas-mediated apoptosis in primary cultured mouse hepatocytes. *Exp Cell Res.* 1994;215:332–337.
18. Moses HL, Yang EY, Pietenpol JA. TGF-beta stimulation and inhibition of cell proliferation: new mechanistic insights. *Cell.* 1990;63:245–247.
19. Postlethwaite AE, Keski-Oja J, Moses HL, Kang AH. Stimulation of the chemotactic migration of human fibroblasts by transforming growth factor beta. *J Exp Med.* 1987;165:251–256.
20. Lu L, Chen SS, Zhang JQ, Ramires FJ, Sun Y. Activation of nuclear factor-kappaB and its proinflammatory mediator cascade in the infarcted rat heart. *Biochem Biophys Res Commun.* 2004;321:879–885.
21. Yin FC. Ventricular wall stress. *Circ Res.* 1981;49:829–842.
22. Gabbiani G. The myofibroblast in wound healing and fibrocontractive diseases. *J Pathol.* 2003;200:500–503.
23. Desmouliere A, Redard M, Darby I, Gabbiani G. Apoptosis mediates the decrease in cellularity during the transition between granulation tissue and scar. *Am J Pathol.* 1995;146:56–66.
24. Takemura G, Ohno M, Hayakawa Y, Misao J, Kanoh M, Ohno A, Uno Y, Minatoguchi S, Fujiwara T, Fujiwara H. Role of apoptosis in the disappearance of infiltrated and proliferated interstitial cells after myocardial infarction. *Circ Res.* 1998;82:1130–1138.
25. Hayakawa K, Takemura G, Kanoh M, Li Y, Koda M, Kawase Y, Maruyama R, Okada H, Minatoguchi S, Fujiwara T, Fujiwara H. Inhibition of granulation tissue cell apoptosis during the subacute stage of myocardial infarction improves cardiac remodeling and dysfunction at the chronic stage. *Circulation.* 2003;108:104–109.
26. Li Y, Takemura G, Kosai K, Takahashi T, Okada H, Miyata S, Yuge K, Nagano S, Esaki M, Khai NC, Goto K, Mikami A, Maruyama R, Minatoguchi S, Fujiwara T, Fujiwara H. Critical roles for the Fas/Fas ligand system in postinfarction ventricular remodeling and heart failure. *Circ Res.* 2004;95:627–636.
27. Hagimoto N, Kuwano K, Inoshima I, Yoshimi M, Nakamura N, Fujita M, Maeyama T, Hara N. TGF-beta 1 as an enhancer of Fas-mediated apoptosis of lung epithelial cells. *J Immunol.* 2002;168:6470–6478.
28. Desmouliere A, Geinoz A, Gabbiani F, Gabbiani G. Transforming growth factor-beta 1 induces alpha-smooth muscle actin expression in granulation tissue myofibroblasts and in quiescent and growing cultured fibroblasts. *J Cell Biol.* 1993;122:103–111.
29. Lefer AM, Ma XL, Weyrich AS, Scalia R. Mechanism of the cardioprotective effect of transforming growth factor beta 1 in feline myocardial ischemia and reperfusion. *Proc Natl Acad Sci U S A.* 1993;90:1018–1022.
30. Chen H, Li D, Saldeen T, Mehta JL. TGF-beta 1 attenuates myocardial ischemia-reperfusion injury via inhibition of upregulation of MMP-1. *Am J Physiol.* 2003;284:H1612–H1617.
31. Grainger DJ. Transforming growth factor beta and atherosclerosis: so far, so good for the protective cytokine hypothesis. *Arterioscler Thromb Vasc Biol.* 2004;24:399–404.
32. Mallat Z, Gojova A, Marchiol-Fournigault C, Esposito B, Kamate C, Merval R, Fradelizi D, Tedgui A. Inhibition of transforming growth factor-beta signaling accelerates atherosclerosis and induces an unstable plaque phenotype in mice. *Circ Res.* 2001;89:930–934.
33. Robertson AK, Rudling M, Zhou X, Gorelik L, Flavell RA, Hansson GK. Disruption of TGF-β signaling in T cells accelerates atherosclerosis. *J Clin Invest.* 2003;112:1342–1350.
34. Reimer KA, Vander Heide RS, Richard VJ. Reperfusion in acute myocardial infarction: effect of timing and modulating factors in experimental models. *Am J Cardiol.* 1993;72:13G–21G.

Available online at www.sciencedirect.com
SCIENCE DIRECT®
Biochemical and Biophysical Research Communications 333 (2005) 562–567
BBRC
www.elsevier.com/locate/ybbrc

Apoptosis signal-regulating kinase 1 is involved not only in apoptosis but also in non-apoptotic cardiomyocyte death

Tetsuya Watanabe [a,1], Kinya Otsu [a,*], Toshihiro Takeda [a,1], Osamu Yamaguchi [a], Shungo Hikoso [a], Kazunori Kashiwase [a], Yoshiharu Higuchi [a], Masayuki Taniike [a], Atsuko Nakai [a], Yasushi Matsumura [b], Kazuhiko Nishida [a,c], Hidenori Ichijo [d], Masatsugu Hori [a]

[a] *Department of Cardiovascular Medicine, Osaka University Graduate School of Medicine, Osaka 565-0871, Japan*
[b] *Department of Medical Information Science, Osaka University Graduate School of Medicine, Osaka 565-0871, Japan*
[c] *Department of Anesthesiology, Osaka University Graduate School of Dentistry, Osaka 565-0781, Japan*
[d] *Laboratory of Cell Signaling, Graduate School of Pharmaceutical Sciences, The University of Tokyo and CREST, Tokyo 113-0033, Japan*

Received 16 April 2005
Available online 6 June 2005

Abstract

The molecular basis of myocardial cell death in the ischemia-reperfused heart still remains to be clarified. Apoptosis signal-regulating kinase 1 (ASK1) is a mitogen-activated protein kinase kinase kinase that plays an important role in stress-induced apoptosis. We studied ASK1$^{-/-}$ mice to examine the role of ASK1 in ischemia–reperfusion injury. In the wild-type heart, ischemia–reperfusion resulted in necrotic injury, whereas infarct size was drastically reduced in the ASK1$^{-/-}$ heart. The necrotic injury was not accompanied with any evidence of apoptosis such as an increase in TUNEL-positive cells, DNA fragmentation or the activation of caspase-3. ASK1$^{-/-}$ cardiomyocytes were more resistant to H_2O_2- or Ca^{2+}-induced apoptotic and non-apoptotic cell death compared with wild-type cells. These data suggest that ASK1 is involved in necrosis as well as apoptosis and that ASK1-dependent necrosis is likely to contribute to myocardial cell death in the ischemia-reperfused heart.

Keywords: ASK1; Ischemia–reperfusion injury; Non-apoptotic cell death

Reperfusion of occluded coronary arteries has become a mainstay of optimal therapeutic intervention for acute myocardial infarction. Paradoxically, reperfusion also results in cell death and scar formation. Therefore, if the reperfusion-induced myocardial injury can be attenuated, then salvage of the myocardium by means of reperfusion therapy could be maximized.

Necrosis and apoptosis are the two major and distinct types of cell death in cardiomyocytes that have been associated with ischemia and reperfusion. Apoptosis is identified in the form of morphological changes such as chromatin condensation, nuclear fragmentation, and formation of apoptotic bodies, all of which are driven by caspases [1]. In contrast, necrosis is primarily manifested either by cell swelling or by rupture of the plasma membrane accompanied by breakdown of organelles [2]. Both necrosis and apoptosis have been reported to be involved in myocardial injury after ischemia–reperfusion [3,4], but the relative contribution of necrosis and apoptosis to ischemia–reperfusion injury remains controversial.

The signal transduction mechanism, by which ischemia–reperfusion leads to cell death, has not yet been fully identified. Recent studies suggest an important role of the mitogen-activated protein (MAP) kinase family in

* Corresponding author. Fax: +81 6 6879 3645.
E-mail address: kotsu@medone.med.osaka-u.ac.jp (K. Otsu).
[1] These authors contributed equally to this work.

0006-291X/$ - see front matter © 2005 Elsevier Inc. All rights reserved.
doi:10.1016/j.bbrc.2005.05.151

ischemia–reperfusion injury [5–7]. Apoptosis signal-regulating kinase 1 (ASK1) is a reactive oxygen species-sensitive MAP kinase kinase kinase, which activates the c-Jun N-terminal kinase (JNK) and p38 MAP kinase [8]. Overexpression of wild-type ASK1 or the constitutively active mutant of ASK1 induces apoptosis in various cells including cardiomyocytes, whereas oxidative stress-induced apoptosis is suppressed in ASK1$^{-/-}$ cells [9–11]. In the study reported here, we used ASK1$^{-/-}$ mice to clarify the in vivo role of ASK1 in ischemia–reperfusion injury. We found that ASK1 plays a pivotal role in the signal transduction pathway mediating non-apoptotic myocardial cell death caused by ischemia–reperfusion.

Materials and methods

This study was carried out under the supervision of the Animal Research Committee in accordance with the Guidelines for Animal Experiments of Osaka University and the Japanese Government's Animal Protection and Management Law (No. 105).

Ischemia–reperfusion studies. The F_6 generation of ASK$^{-/-}$ mice with a C57Bl6/J background was described previously [11]. Ischemia–reperfusion studies were performed as we described previously [5,12]. The 8- to 10-week-old mice were anesthetized with sodium pentobarbital (50 mg/kg, intraperitoneal injection). After a midsternal thoracotomy, silk thread (8-0 type) was passed around the left coronary artery (LCA) about 1 mm distal from the tip of the left auricle and made into an occlusive snare. Following a 30 min ligation of the LCA, the snare was released for 2 h. Body temperature was monitored with a rectal probe connected to a digital thermometer and was maintained as close as possible to 37 °C throughout the experiment with the aid of a heating pad and heat lamps. Then, the LCA was re-occluded at the same point and Evans blue dye was infused from the left ventricular cavity. The heart was cut transversely into five sections, which were then incubated in a 1.0% solution of triphenyltetrazolium chloride (TTC) for 20 min at 37 °C. The area at risk was defined as the ratio of the area of the ischemic region to the left ventricular area and the infarct size as the ratio of the area of the infarct region to that of the ischemic region.

Histological analysis and evaluation of apoptosis. The heart samples were fixed immediately with buffered 3.7% formalin, embedded in paraffin, and cut into 3-μm slices. Paraffin-embedded heart sections were subjected to the the terminal deoxynucleotidyl transferase biotin–dUTP nick end labeling (TUNEL) assay using an in situ apoptosis detection kit (Takara, Otsu, Japan).

Isolation of ventricular myocytes and survival assay. Ventricular myocytes from 1- to 2-day-old mice were prepared as described previously [9]. Cardiomyocytes were treated with H_2O_2 or ionomycin for 24 h. A 3-(4,5-dimethylthiazol-2-yl)-2,5-diphenyltetrazolium bromide (MTT) assay-based Cell Counting kit-8 (Dojindo, Kumamoto, Japan) was used to determine the number of surviving cells in triplicate. Cells were stained by incubation with Hoechst 33258 (1 mM) or with fluorescent conjugate Annexin V and propidium iodide (PI) (Annexin V-FITC Apoptosis Detection Kit, BioVision Research Products, Mountain View, CA, USA).

In vitro kinase assay and Western blots. The activity of ASK1 was measured by an immune complex kinase assay as described previously [9]. Immunoprecipitation of endogenous ASK1 was performed on 250 μg of myocardial extracts with anti-ASK1 antibody (Santa Cruz Biotechnology, Santa Cruz, CA, USA), followed by measurement of the immune complex kinase activity using MKK6 as a substrate. Total protein homogenates (50 μg for p38 and JNK, 20 μg for ERK) were subjected to Western blot analysis using the antibodies against mouse p38 (C-20), JNK1 (FL), and ERK1 (K-23) from Santa Cruz Biotechnology and phospho-p38, phospho-JNK, phospho-ERK, and cleaved-caspase-3 from Cell Signaling Technology (Beverly, MA, USA). Western blots were developed with the enhanced chemiluminescence kit (Amersham Pharmacia, Piscataway, NJ, USA). Signals were quantified by means of densitometry of scanned autoradiographs using Scion Image software (version 4.02; Scion, Fredrick, MD, USA). All values are representative of 4–6 animals per treatment group for each time point.

The DNA ladder assay. The presence of a DNA ladder was detected by using agarose gel electrophoresis as described elsewhere [13]. Tissue samples were quickly homogenized, digested with proteinase K, and incubated with RNase A.

Statistical analysis. Results are shown as means ± SEM. Paired data were evaluated by Student's t test. A one-way ANOVA with the Bonferroni's post hoc test or repeated measures ANOVA was used for multiple comparisons. A value of $p < 0.05$ was considered statistically significant.

Results

The ASK$^{-/-}$ mice with a C57Bl6/J mice background appeared phenotypically normal and had a normal global cardiac structure and function, when compared with age-matched C57Bl6/J wild-type mice (WT) [9]. To examine the effect of ASK1 ablation on ischemia–reperfusion injury, WT and ASK$^{-/-}$ mice were subjected to 30 min of LCA occlusion followed by 2 h of reperfusion. No significant differences among the groups were observed in terms of the rate-pressure product or in the rectal temperature during the ischemia–reperfusion procedure (data not shown). The areas at risk, identified by a lack of Evans blue stain, in the ASK$^{-/-}$ and WT hearts (56.3 ± 4.6% and 57.5 ± 5.1%) were not significantly different (Fig. 1). In WT hearts, ischemia–reperfusion resulted in significant necrotic injury, as evidenced

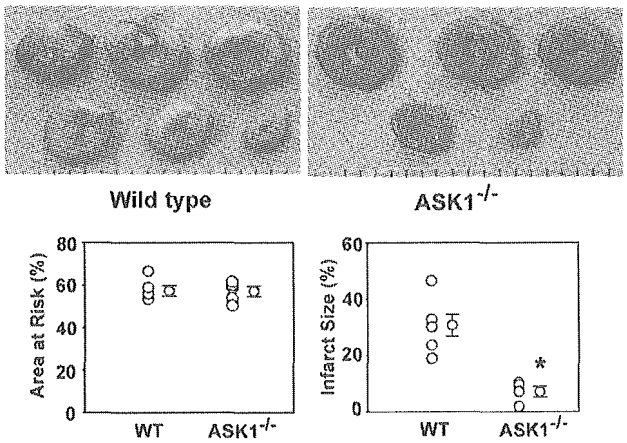

Fig. 1. The size of the myocardial infarct in WT and ASK$^{-/-}$ subjected to ischemia–reperfusion. The upper panel shows representative images of heart slices double-stained with Evans blue and TTC. The lower panel shows the size of the ischemic area at risk and of the infarct in mouse hearts subjected to ischemia–reperfusion ($n = 5$ for each group).

by a large area of negative TTC staining (32.4 ± 11.3% of area at risk). In $ASK^{-/-}$, on the other hand, the infarct was limited to the region close to the LCA origin where the silk thread was passed around the LCA and the infarct size was substantially smaller at 7.6 ± 3.5% ($p < 0.01$) (Fig. 1).

Next, we examined whether ischemia–reperfusion injury was accompanied by the activation of ASK1, by measuring ASK1 activity in hearts during ischemia and reperfusion. In WT hearts, 5 min of ischemia resulted in an increase in ASK1 activity, and additional increase was detected upon reperfusion (Fig. 2A). Activation of ASK1 remained above the baseline level after 30 min of ischemia followed by 30 min of reperfusion. There were differences neither in the basal protein levels of p38, JNK, and ERK in $ASK^{-/-}$ and WT hearts, nor in the basal levels of phosphorylated p38, JNK, and ERK (Figs. 2B and C). In WT hearts, a biphasic increase was observed in the level of phosphorylated p38 after ischemia and ischemia–reperfusion, while both the peaks were significantly attenuated in $ASK^{-/-}$ hearts. We also examined the phosphorylation state of JNK. In WT hearts, ischemia–reperfusion produced a significant increase in the phosphorylation level of both isoforms of JNK, p46, and p54, while this increase was significantly smaller in $ASK^{-/-}$ hearts. On the other hand, the phosphorylation state of both isoforms of ERK, p44 and p46, showed no significant difference between WT and $ASK^{-/-}$ (Fig. 2C).

We also assessed the role of apoptosis in cardiomyocyte death induced by ischemia–reperfusion injury. The number of TUNEL-positive cells in WT and $ASK^{-/-}$ was not significantly different either at the baseline or at the end of reperfusion (27.5 ± 7.8 cells/10^5 myocytes in WT control hearts and 33.1 ± 13.3 cells/10^5 myocytes in WT hearts after 120 min of reperfusion; 31.9 ± 7.9 cells/10^5 myocytes in $ASK^{-/-}$ control hearts and 35.3 ± 12.0 cells/10^5 myocytes in $ASK^{-/-}$ hearts after 120 min of reperfusion). DNA nucleosomal fragmentation of cardiomyocytes was evaluated in the non-ischemic and ischemic zones of both the groups (Fig. 3B). No visible DNA ladders were observed either at the baseline or after 120 min of reperfusion (WT and $ASK^{-/-}$). Western blot analysis using polyclonal caspase-3 antibody, which recognizes active caspase-3, was performed to evaluate caspase-3 activation. Although active caspase-3 was detected in positive control (cytosolic extract from apoptotic Jurkat cells), it was not detected either at baseline or during ischemia–reperfusion in either WT or $ASK^{-/-}$ hearts (Fig. 3C).

The generation of reactive oxygen species and Ca^{2+} overload is known to play a pivotal role in the pathogenesis of ischemia–reperfusion injury [14]. We assessed whether ASK1 is required for H_2O_2- or ionomycin-induced cardiomyocyte death, by using neonatal cardiomyocytes derived from WT and $ASK^{-/-}$ hearts (Fig. 4A). $ASK^{-/-}$ cardiomyocytes were more resistant than WT cells to H_2O_2 or ionomycin as determined with

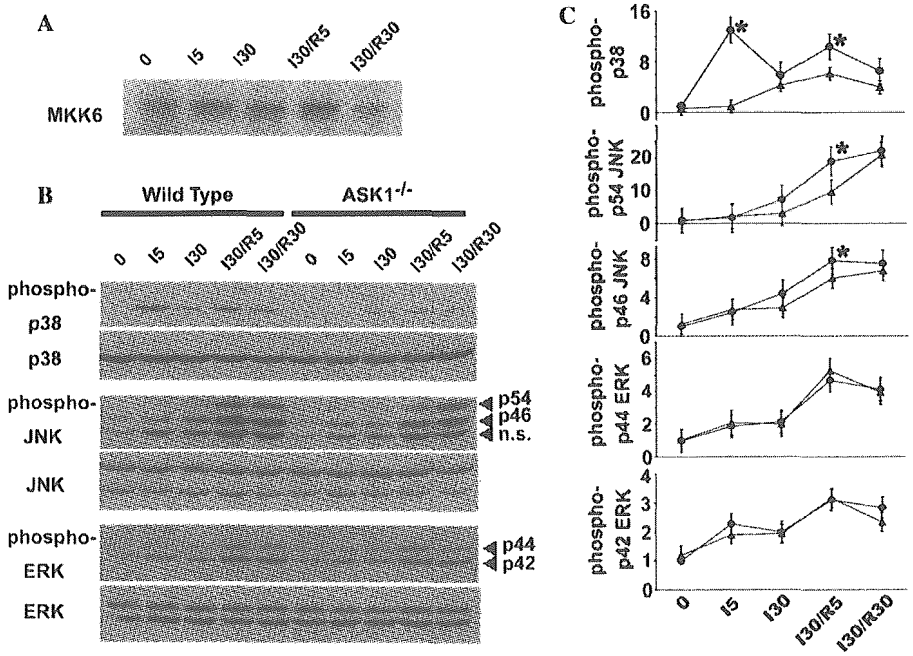

Fig. 2. The activation of ASK1, p38, JNK, and ERK in WT and $ASK^{-/-}$ hearts after ischemia and reperfusion. (A) ASK1 activity was measured in an immune complex assay, using His-MKK6 as a substrate. This panel shows representative image of ASK1 activation. I5, ischemia for 5 min; I30, ischemia for 30 min; I30/R5, ischemia for 30 min and reperfusion for 5 min; I30/R30, ischemia for 30 min and reperfusion for 30 min. (B) The activity of p38, JNK, and ERK was assessed by means of immunoblotting with anti-phospho-specific antibody after ischemia and reperfusion. The filters were reprobed with anti-nonphospho-specific antibody. (C) Densitometric analysis upon p38, p54 JNK, p46 JNK, p44 ERK, and p42 ERK phosphorylation. *$p < 0.05$ vs $ASK^{-/-}$ at the corresponding time points ($n = 4$–6 for each time point).

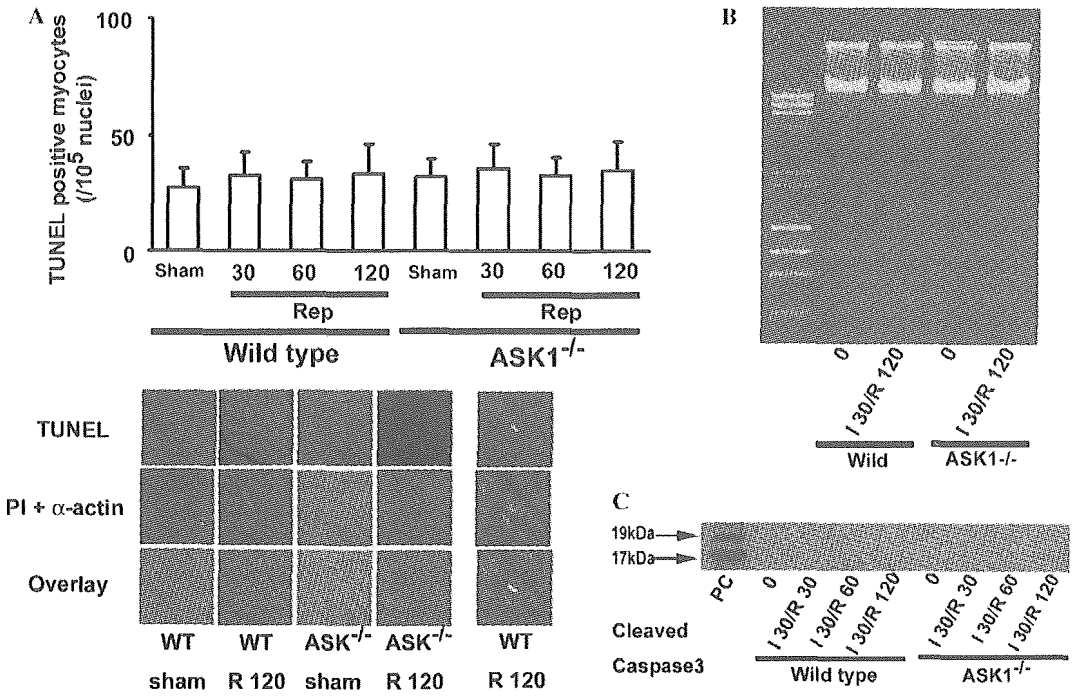

Fig. 3. Apoptosis in WT and $ASK^{-/-}$ subjected to ischemia–reperfusion. (A) Number of TUNEL-positive cells in WT and $ASK^{-/-}$ hearts subjected to ischemia–reperfusion. The durations of reperfusion was 30, 60 or 120 min. Lower panels show representative images. (B) DNA fragmentation in WT and $ASK^{-/-}$ hearts after 30 min ischemia followed by 120 min reperfusion. (C) Analysis of cleaved caspase-3 protein levels in cardiac tissue after ischemia–reperfusion. Immunoblotting was performed with anti-cleaved caspase-3 antibody.

an MTT assay (Fig. 4A). To characterize cell death induced by H_2O_2 or ionomycin, the nuclear morphology of the cells stained with Hoechst dye 33258 was examined. We found that WT cardiomyocytes subjected to H_2O_2 or ionomycin reproducibly showed nuclear shrinkage (Fig. 4B). Nuclear shrinkage is known to be associated with caspase-independent cell death [15]. These dead cells exhibited PI-positive and Annexin V-negative staining, indicating non-apoptotic cell death. Furthermore, apoptotic cell death was also induced by H_2O_2 or ionomycin as determined by nuclear fragmentation or chromatin condensation in WT cardiomyocytes (Fig. 4B, insets). The number of the apoptotic cells was less than 10% relative to that of cells showing nuclear shrinkage. We determined that both the forms of cell death were drastically reduced in $ASK^{-/-}$ cardiomyocytes.

Discussion

This is the first study to evaluate the involvement of ASK1 in myocardial ischemia–reperfusion injury. Our results indicate that ASK1 plays a pivotal role in the signal transduction pathway mediating myocardial cell death caused by ischemia–reperfusion. ASK1 reportedly induces apoptosis in various cells through mitochondria-dependent caspase activation [8,11,16]. In the mouse ischemia–reperfusion model used in our report, however, we could not detect any evidence of cardiomyocyte apoptosis induced by 30 min ischemia followed by 2 h reperfusion. Although apoptosis may contribute to some extent to the exacerbation of myocardial injury [4], the major type of cardiomyocyte death after ischemia–reperfusion is thought to be necrosis [13,17–19]. Since previously reported studies of cell death and ischemia–reperfusion injury show major disparities in experimental animals, models, protocols, and methods used to determine apoptosis in its various stages [3], it is difficult to estimate the extent of necrosis and apoptosis induced by ischemia–reperfusion. During the time of our experiment, ischemia–reperfusion resulted in a large area of negative TTC staining, a marker of necrotic injury, in WT hearts, whereas it was drastically reduced in $ASK^{-/-}$ hearts. We recently used the same experimental protocol as employed in the study presented here to demonstrate that the cyclophilin D-dependent mitochondrial permeability transition regulates necrotic cell death, but not apoptotic cell death, and that it is a critical event in ischemia–reperfusion injury [12]. Therefore, we can conclude that ASK1 is involved in necrotic cardiomyocyte death related to ischemia–reperfusion injury. The involvement of ASK1 in necrotic cell death was confirmed by the in vitro study, in which we were able to show that $ASK^{-/-}$ cardiomyocytes were resistant to H_2O_2 or ionomycin in both apoptotic and non-apoptotic cell death. Nuclear shrinkage has previously been identified as a feature of hypoxic or ischemic caspase-independent cell death associated with swelling of

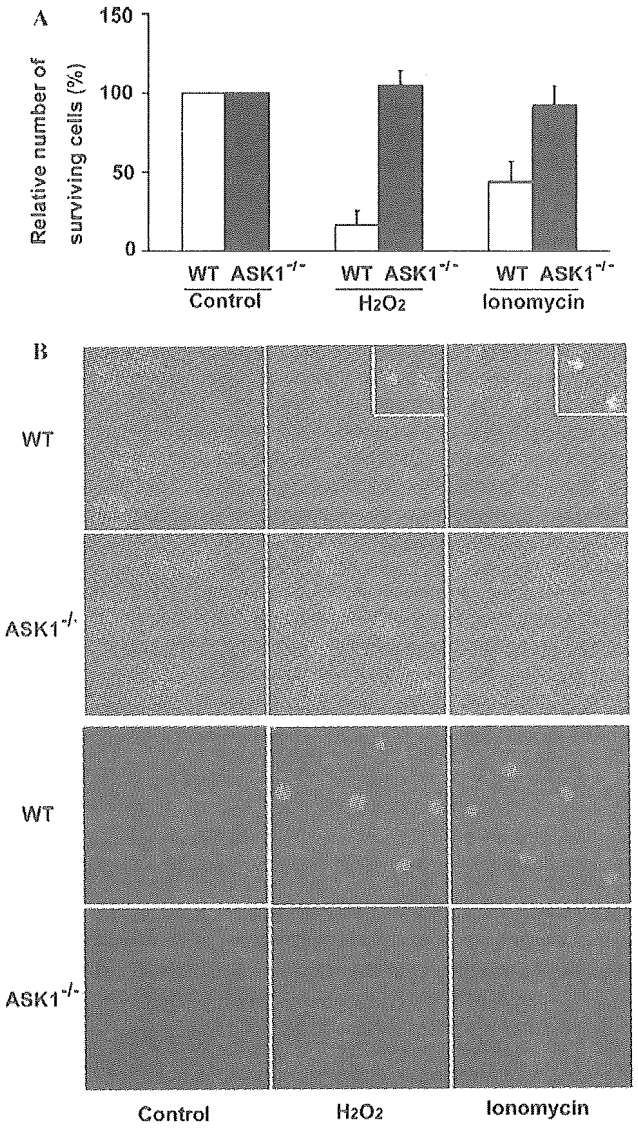

Fig. 4. Involvement of ASK1 in apoptosis and non-apoptotic cell death in cardiomyocytes. (A) Cell viability was assessed with a Cell Counting kit. Data show means ± SEM of three independent experiments using different cell preparations. Viability of cells is expressed as the percentage viability of cells in the absence of H_2O_2 or ionomycin after incubation of neonatal cardiomyocytes isolated from WT and $ASK^{-/-}$ were incubated with 100 μM H_2O_2 or 0.25 μM ionomycin for 24 h. (B) $ASK^{-/-}$ or WT neonatal cardiomyocytes treated with 100 μM H_2O_2 or 0.25 μM ionomycin for 24 h were stained with Hoechst 33258 (upper 2 rows) or with propidium iodide and fluorescent conjugate of Annexin V (lower 2 rows). (Insets) Cells showing the condensed chromatin and fragmented nuclei, which are the morphological characteristics of apoptosis.

organelles, vacuolization, and increased membrane permeability [20,21]. Various types of cells exposed to hypoxia developed significant nuclear shrinkage [15], which, although not a universal phenomenon in all types of caspase-independent cell death, is a feature of some kinds of caspase-independent cell death. It has further been reported that ASK1 has a kinase-independent killing function in caspase-independent cell death, leading to a nuclear crumpling morphology distinct from apoptotic cell death [22] and also distinct from the nuclear shrinkage observed in this study. It appears therefore that ASK1 may play a role in each form of cell death, apoptosis, crumpling cell death, and cell death associated with nuclear shrinkage. However, we could not rule out the possibility that ASK1-dependent apoptotic cardiomyocyte death was involved in ischemia–reperfusion injury for the following reasons: (1) As the time course of the apoptotic cascade and the time interval needed until the occurrence of DNA fragmentation remain uncertain, 30 min of ischemia followed by 2 h reperfusion used in our study might not be sufficient to induce cardiomyocyte apoptosis. (2) It is unclear whether apoptotic cardiomyocytes progress to necrotic cell death. (3) The beginning of the apoptotic cascade could not be detected due to the limitations of the method used.

Previous studies have demonstrated that ASK1 can induce a caspase-dependent apoptosis pathway through its kinase activity [16]. Our study found that ASK1 activity was elevated after ischemia and ischemia with reperfusion. It has been reported that ASK1 mediates apoptosis with sustained activation of JNK/p38 [11]. However, it is not clear whether sustained activation of JNK/p38 is required for ASK1-dependent necrosis. In reperfused WT hearts, p38 and JNK were activated, but they were significantly reduced in $ASK^{-/-}$ hearts. We previously showed that disruption of a single copy of the p38α gene decreased the extent of the infarct after ischemia–reperfusion [5]. The lower level of phosphorylated p38 in $ASK^{-/-}$ hearts may thus be involved in the cardioprotective mechanism.

The results of our study demonstrated the existence of a novel mechanism of cell death signaling by ASK1. It remains unknown, however, whether this process involves the kinase activity of ASK1. Further investigations are needed for the precise characterization of the molecular mechanism, which determines the role of ASK1 in non-apoptotic cardiomyocyte death.

Acknowledgments

We are grateful to Ms. Sunao Tanaka for expert technical assistance. This work was supported by a Grant-in-Aid for Scientific Research from the Ministry of Education, Culture, Sports, Science and Technology, Japan (16590683), and Research grant from Takeda Science Foundation (to K.O.).

References

[1] G.S. Salvesen, V.M. Dixit, Caspases: intracellular signaling by proteolysis, Cell 91 (1997) 443–446.
[2] Z.Q. Zhao, Oxidative stress-elicited myocardial apoptosis during reperfusion, Curr. Opin. Pharmacol. 4 (2004) 159–165.

[3] A. Elsasser, K. Suzuki, S. Lorenz-Meyer, C. Bode, J. Schaper, The role of apoptosis in myocardial ischemia: a critical appraisal, Basic Res. Cardiol. 96 (2001) 219–226.
[4] F. Eefting, B. Rensing, J. Wigman, W.J. Pannekoek, W.M. Liu, M.J. Cramer, D.J. Lips, P.A. Doevendans, Role of apoptosis in reperfusion injury, Cardiovascl. Res. 61 (2004) 414–426.
[5] K. Otsu, N. Yamashita, K. Nishida, S. Hirotani, O. Yamaguchi, T. Watanabe, S. Hikoso, Y. Higuchi, Y. Matsumura, M. Maruyama, T. Sudo, H. Osada, M. Hori, Disruption of a single copy of the p38α MAP kinase gene leads to cardioprotection against ischemia–reperfusion, Biochem. Biophys. Res. Commun. 302 (2003) 56–60.
[6] C.M. Pombo, J.V. Bonventre, J. Avruch, J.R. Woodgett, J.M. Kyriakis, T. Force, The stress-activated protein kinases are major c-Jun amino-terminal kinases activated by ischemia and reperfusion, J. Biol. Chem. 269 (1994) 26546–26551.
[7] M.A. Bogoyevitch, J. Gillespie-Brown, A.J. Ketterman, S.J. Fuller, R. Ben-Levy, A. Ashworth, C.J. Marshall, P.H. Sugden, Stimulation of the stress-activated mitogen-activated protein kinase subfamilies in perfused heart. p38/RK mitogen-activated protein kinases and c-Jun N-terminal kinases are activated by ischemia/reperfusion, Circ. Res. 79 (1996) 162–173.
[8] H. Ichijo, E. Nishida, K. Irie, P. ten Dijke, M. Saitoh, T. Moriguchi, M. Takagi, K. Matsumoto, K. Miyazono, Y. Gotoh, Induction of apoptosis by ASK1, a mammalian MAPKKK that activates SAPK/JNK and p38 signaling pathways, Science 275 (1997) 90–94.
[9] O. Yamaguchi, Y. Higuchi, S. Hirotani, K. Kashiwase, H. Nakayama, S. Hikoso, T. Takeda, T. Watanabe, M. Asahi, M. Taniike, Y. Matsumura, I. Tsujimoto, K. Hongo, Y. Kusakari, S. Kurihara, K. Nishida, H. Ichijo, M. Hori, K. Otsu, Targeted deletion of apoptosis signal-regulating kinase1 attenuates left ventricular remodeling, Proc. Natl. Acad. Sci. USA 100 (2003) 15883–15888.
[10] M. Saitoh, H. Nishitoh, M. Fujii, K. Takeda, K. Tobiume, Y. Sawada, M. Kawabata, K. Miyazono, H. Ichijo, Mammalian thioredoxin is a direct inhibitor of apoptosis signal-regulating kinase (ASK) 1, EMBO J. 17 (1998) 2596–2606.
[11] K. Tobiume, A. Matsuzawa, T. Takahashi, H. Nishitoh, K. Morita, K. Takeda, O. Minowa, K. Miyazono, T. Noda, H. Ichijo, ASK1 is required for sustained activations of JNK/p38 MAP kinases and apoptosis, EMBO Rep. 2 (2001) 222–228.
[12] T. Nakagawa, Y. Shimizu, T. Watanabe, O. Yamaguchi, K. Otsu, H. Yamagata, H. Inohara, T. Kubo, Y. Tsujimoto, The mitochondrial permeability transition dependent on cyclophilin D regulates some forms of necrotic death, but not apoptotic cell death, Nature 434 (2005) 652–658.
[13] Z.-Q. Zhao, C.D. Morris, J.M. Budde, N.-P. Wang, S. Muraki, H.Y. Sun, R.A. Guyton, Inhibition of myocardial apoptosis reduces infarct size and improves regional contractile dysfunction during reperfusion, Cardiovasc. Res. 59 (2003) 132–142.
[14] J.N. Weiss, P. Korge, H.M. Honda, P. Ping, Role of the mitochondrial permeability transition in myocardial disease, Circ. Res. 93 (2003) 292–301.
[15] K. Shinzawa, Y. Tsujimoto, PLA2 activity is required for nuclear shrinkage in caspase-independent cell death, J. Cell Biol. 163 (2003) 1219–1230.
[16] T. Hatai, A. Matsuzawa, S. Inoshita, Y. Mochida, T. Kuroda, K. Sakamaki, K. Kuida, S. Yonehara, H. Ichijo, K. Takeda, Execution of apoptosis signal-regulating kinase 1 (ASK1)-induced apoptosis by the mitochondria-dependent caspase activation, J. Biol. Chem. 275 (2000) 26576–26581.
[17] E. Hochhauser, S. Kivity, D. Offen, N. Maulik, H. Otani, Y. Barhum, H. Pannet, V. Shneyvays, A. Shainberg, V. Goldshtaub, A. Tobar, B.A. Vidne, Bax ablation protects against myocardial ischemia–reperfusion injury in transgenic mice, Am. J. Physiol. Heart Circ. Physiol. 284 (2003) H2351–H2359.
[18] X.L. Ma, S. Kumar, F. Gao, C.S. Louden, B.L. Lopez, T.A. Christopher, C. Wang, J.C. Lee, G.Z. Feuerstein, T.L. Yue, Inhibition of p38 mitogen-activated protein kinase decreases cardiomyocyte apoptosis and improves cardiac function after myocardial ischemia and reperfusion, Circulation 99 (1999) 1685–1691.
[19] J.D. McCully, H. Wakiyama, Y.-J. Hsieh, M. Jones, S. Levitsky, Differential contribution of necrosis and apoptosis in myocardial ischemia–reperfusion injury, Am. J. Physiol. Heart Circ. Physiol. 286 (2004) H1923–H1935.
[20] T. Grune, K. Muller, S. Zollner, R. Haseloff, I. Blasig, H. David, W. Siems, Evaluation of purine nucleotide loss, lipid peroxidation and ultrastructural alterations in post-hypoxic hepatocytes, J. Physiol. Lond. 498 (1997) 511–522.
[21] K.-A. Hossmann, U. Oschlies, W. Schwindt, H. Krep, Electron microscopic investigation of rat brain after brief cardiac arrest, Acta Neuropathol. 101 (2001) 101–113.
[22] S.J. Charette, H. Lambert, J. Landry, A kinase-independent function of Ask1 in caspase-independent cell death, J. Biol. Chem. 276 (2001) 36071–36074.

Circulation Research
JOURNAL OF THE AMERICAN HEART ASSOCIATION

American Heart Association®
Learn and Live℠

Hepatitis C Virus Infection and Cardiomyopathies

Akira Matsumori

Circ. Res. 2005;96;144-147
DOI: 10.1161/01.RES.0000156077.54903.67
Circulation Research is published by the American Heart Association. 7272 Greenville Avenue, Dallas, TX 72514
 Print ISSN: 0039-2499. Online ISSN: 1524-4628

See related article, pages 148–150

Hepatitis C Virus Infection and Cardiomyopathies

Akira Matsumori

Cardiomyopathies may present as idiopathic dilated, hypertrophic, or restrictive disease, arrhythmogenic right ventricular cardiomyopathy (ARVC), and various other distinct disorders of the heart muscle.[1] They constitute a heterogeneous group of myocardial diseases of multifactorial etiologies, including genetic anomalies and acquired immune factors, such as viral infections. The myocardium may be infected by a wide variety of viruses, although most commonly by enteroviruses, coxsackievirus B in particular. However, in many cases, when myocarditis has been diagnosed on the basis of clinical manifestations, a viral origin cannot be confirmed, despite extensive laboratory investigations.

The clinical presentation of viral myocarditis is variable. When myocardial necrosis is diffuse, congestive heart failure develops, and growing evidence now links viral myocarditis with dilated cardiomyopathy.[2,3] Localized myocardial lesions may result in thinning or aneurysms of the ventricular wall which, in the case of ARVC, are complicated by arrhythmias.[4] When myocardial necrosis is limited to the subendocardium, restrictive cardiomyopathy may develop. Finally, although it has not been established that hypertrophic cardiomyopathy is a complication of viral myocarditis, asymmetrical septal hypertrophy has been observed in some patients with myocarditis.[5]

A high prevalence of hepatitis C virus (HCV) infection has recently been noted in patients with hypertrophic cardiomyopathy, dilated cardiomyopathy, and myocarditis (Figure 1).[6–15] In this issue of *Circulation Research*, Omura et al[16] report that mice transgenic for the HCV-core gene develop ventricular dilatation, cardiac dysfunction, and myocardial fibrosis at 12 months, similar to the pathological manifestations observed in human dilated cardiomyopathy. Although HCV infection may be the cause of several phenotypically different cardiomyopathies, mild inflammation with mononuclear cell infiltration has also been observed with HCV infection in humans.[6,7,9] However, no lymphocytic infiltration was observed in these HCV-core transgenic mice. Furthermore, cardiomyocyte hypertrophy and disarray of the myofibers are typical characteristics of human hypertrophic cardiomyopathy, but the wall thickness of the HCV-core mice was not increased. Therefore, although the HCV-core mice did not have all the phenotypical manifestations of human cardiomyopathies, the observations made by Omura et al are nevertheless relevant, because they show that the expression of the HCV-core is associated with the long-term development of myocardial disease. They also found that the expression of atrial and brain natriuretic polypeptides was enhanced, and that activator protein-1 (AP-1) was activated in the heart. However, nuclear factor-κB (NF-κB) was not activated. The authors state that the activation of myocardial AP-1 by HCV-core is an important pathway toward cardiomyopathic changes, although it has not been shown that blocking this pathway changes the disease phenotype. Whereas AP-1 is activated in transgenic mice of HCV core protein,[17] the latter interferes with the activation of AP-1 in human macrophages.[18] Furthermore, HCV core protein inhibits AP-1,[19] and activates extracellular signal-regulated kinase (ERK), C-jun N-terminal kinase (JNK), and p38 mitogen-activated protein (MAP) kinase.[20] Although, HCV core protein is known to activate NF-κB,[21] the authors found no changes in NF-κB. Therefore, further studies will be necessary to clarify the molecular pathogenetic changes observed in HCV-core transgenic mice.

Phenotypes of HCV Cardiomyopathies

In a collaborative research project of the Committees for the Study of Idiopathic Cardiomyopathy in Japan,[22] HCV antibodies were found in 74 of 697 patients (10.6%) with hypertrophic cardiomyopathy and in 42 of 633 patients (6.3%) with dilated cardiomyopathy, significantly more prevalent than the 2.4% observed in age-matched volunteer blood donors in Japan. In an initial study, we evaluated 31 patients with cardiomyopathy and myocarditis and found HCV RNA by polymerase chain reaction in the hearts of 6 patients (19.4%) with dilated cardiomyopathy.[6] Over a 10-year period, we identified 19 among 191 patients with dilated cardiomyopathy (9.9%) who had evidence of HCV infection, in contrast to only 1 of 40 patients with ischemic heart disease (2.5%). No patient with dilated cardiomyopathy and positive HCV antibody had a history of blood transfusion or intravenous drug use, three had a history of hepatitis, mildly elevated serum amino-transferase were present in 10, and nine patients had normal liver function tests. The main clinical manifestations at initial presentation were heart failure and cardiac arrhythmias. Among these patients with HCV antibodies, 10 had HCV RNA in the serum, and six patients had type 1b HCV. HCV RNA was found in the heart of eight patients, and negative strands of HCV RNA were detected in the heart of two patients.[23] Because negative RNA molecules are intermediates in the replication of the HCV genome, we presume that HCV replicates in myocardial tissues.

From the Department of Cardiovascular Medicine, Kyoto University Graduate School of Medicine, Kyoto, Japan.

Correspondence to Akira Matsumori, MD, PhD, Department of Cardiovascular Medicine, Kyoto University Graduate School of Medicine, 54 Kawahara-cho Shogoin, Sakyo-ku, Kyoto 606-8507, Japan. E-mail amat@kuhp.kyoto-u.ac.jp

(*Circ Res.* 2005;96:144-147.)

***Circulation Research* is available at http://www.circresaha.org**
DOI: 10.1161/01.RES.0000156077.54903.67

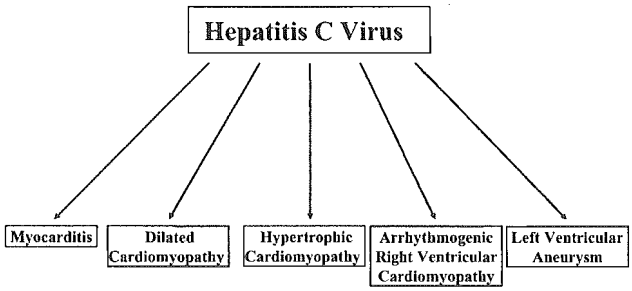

Figure 1. Hepatitis C virus causes various heart diseases.

During the same period, we identified 16 of 113 patients with hypertrophic cardiomyopathy (14.1%) with evidence of HCV infection. None of these 16 patients had a family history of hypertrophic cardiomyopathy. Seven patients had hepatomas, four had received blood transfusions, and 10 patients had mildly elevated serum amino-transferase. Apical hypertrophic cardiomyopathy was diagnosed in nine patients who had ace of spade–shaped deformities of the left ventricle, with an apical/mid anterior free wall thickness ratio >1.3. Histopathological studies showed mild to severe degrees of myocyte hypertrophy in the right or left ventricle, mild to moderate fibrosis, and mild cellular infiltration. Type 1b HCV RNA was detected in the serum of seven patients, HCV RNA in biopsy specimens of six, and negative strands of hepatitis C virus RNA in the biopsied hearts of two patients. Analysis by fluorescent single-stand conformation polymorphism showed the presence of multiple clones in the sera of patients with hypertrophic cardiomyopathy.[23] Teragaki and coworkers[24] recently found 18 of 80 Japanese patients with hypertrophic cardiomyopathy (22.5%) with positive HCV antibodies, a prevalence significantly higher than in controls, and higher than in our study. In their study, seven patients had type 1b, and five patients had type 2a HCV.

Prolonged Persistence of Hepatitis C Virus Genomes in Paraffin-Embedded Hearts

A multicenter study was conducted by the Scientific Council on Cardiomyopathies of the World Heart Federation (Bernhard Maisch, MD, Chairman) to test the reproducibility of detection of viral genomes, such as enteroviruses, adenovirus, cytomegalovirus, and HCV in formalin-fixed tissues. The autopsy and biopsy materials were analyzed blindly. We found HCV genomes in 2 of 11 hearts (18%) of patients with dilated cardiomyopathy and myocarditis from Italy, and in 4 of 11 hearts (36%) from the United States, two from patients with myocarditis and two with ARVC,[23] which suggests that HCV may cause ARVC. Because the detection of HCV genomes in formalin-fixed sections is less sensitive than in frozen sections, HCV infection may be a more common cause of myocardial diseases.

In collaboration with the National Cardiovascular Center and Juntendo University, we have detected HCV RNA in paraffin sections of autopsied hearts from six patients with hypertrophic cardiomyopathy (26.0%), three patients with dilated cardiomyopathy (11.5%), and four patients with myocarditis (33.3%). These samples were harvested between 1979 and 1990, confirming that HCV RNA can be amplified from paraffin-embedded hearts preserved for many years.[14] We also examined autopsied hearts from patients with dilated cardiomyopathy in a collaborative study with the University of Utah and found HCV RNA in 8 of 23 hearts (35%) with positive actin genes. The sequences of HCV genomes recovered from these hearts were highly homologous to the standard strain of HCV.[23] However, the rates of HCV genomes detection in the hearts of patients with cardiomyopathies varied widely among different regions of the world. For example, no HCV genome was detected among 24 hearts obtained from St Paul's Hospital, in Vancouver, Canada. These observations suggest that the frequency of cardiomyopathy caused by HCV infection may be different in different regions or different populations. Some European investigators have even reported negative associations between HCV infection and dilated cardiomyopathy, although these discordant results may be attributable to inappropriate controls, incomplete clinical investigation, or other factors such as regional or racial differences.

We have recently analyzed sera stored during the Myocarditis Treatment Trial[25] of immunosuppression in patients with heart failure and myocarditis. Anti-HCV antibodies were identified in 59 of 1355 patients (4.4%), including 6 of 102 patients (5.9%) with biopsy-proven myocarditis, and 53 of 1253 patients (4.2%) whose biopsy specimens did not satisfy the Dallas criteria. Because, according to the US Center for Disease Control, the prevalence of HCV infection in the general US population is 1.8%,[26] HCV infection is more prevalent in patients with heart failure because of myocarditis. Furthermore, variations between 0% and 15% were found in the prevalence of HCV infection among the different medical centers and regions.[27] Thus, anti-HCV antibodies were recoverable in sera stored for 13 to 17 years and were more prevalent in patients with myocarditis and heart failure than in the general population. In regions where its prevalence is high, HCV infection may be an important cause of myocarditis and heart failure.

Genes of the Major Histocompability Complex Class II May Influence the Development of Different Phenotypes of HCV Cardiomyopathies

The human major histocompatibility complex (MHC) is located on the short arm of chromosome 6 and encodes for several protein products involved in immune function, including complement, TNF-α, and the human leukocyte antigen (HLA) complex, the polymorphisms of which are often proposed as determinants for the susceptibility to various diseases. Recent studies on HCV hepatitis showed that DQB1*0301 was associated with clearance of the virus. DRB1*1101, which is also in linkage disequilibrium with DQB1*0301, was associated with clearance. Several other studies have examined the association of MHC alleles with the progression of liver disease, and DQB1*0401 and DRB1*0405 were more prevalent among patients who developed chronic liver disease. We have recently performed association analyses of alleles distributions, using frequencies of phenotype in patients with hypertrophic or dilated cardiomyopathy. The frequency prevalence of HLA-DQB1*0303 and HLA-DRB1*0901 was most prominently increased in

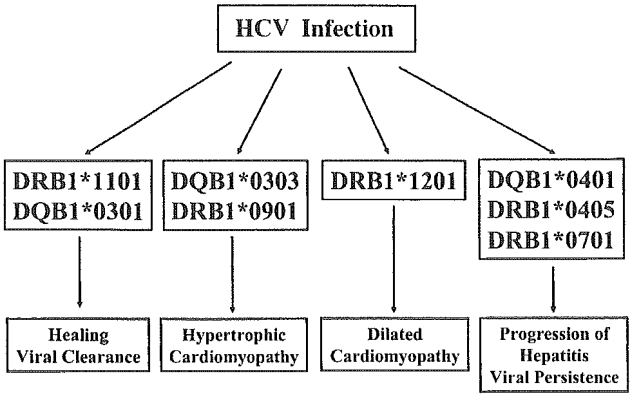

Figure 2. Major histocompatibility complex genes and HCV infection.

patients with hypertrophic cardiomyopathy. In contrast, there was no increase in either allele in patients experiencing dilated cardiomyopathy. HLA-DRB1*1201 was slightly increased in patients with dilated cardiomyopathy, but not in patients with hypertrophic disease (Figure 2).[15] MHC class II genes may play a role in the clearance of, and susceptibility to HCV infection, and may influence the development of different phenotypes of cardiomyopathy.

Treatment of HCV Cardiomyopathies

In patients with HCV hepatitis, the success of treatment can be measured by the biochemical and virological responses. However, therapeutic markers have not been introduced in clinical practice to follow HCV cardiomyopathies. We have examined the effects of interferon on myocardial injury associated with active HCV hepatitis in collaboration with colleagues from Shimane University.[11] We used TL-201-SPECT, because it is more sensitive than electrocardiography or echocardiography to detect myocardial injury induced by HCV. The SPECT scores decreased in 8 of 15 patients (53%) in whom interferon treatment was completed. Circulating HCV disappeared after interferon therapy in all patients who had either a decrease or no change in SPECT scores, and HCV genomes persisted in the blood of two patients whose clinical status worsened.[11] This preliminary study suggests that interferon is a promising treatment for myocardial diseases caused by HCV. We have also reported the treatment with interferon guided by serial measurements of serum HCV RNA and cardiac troponin T in a patient presenting with dilated cardiomyopathy and striated myopathy attributable to HCV infection.[12]

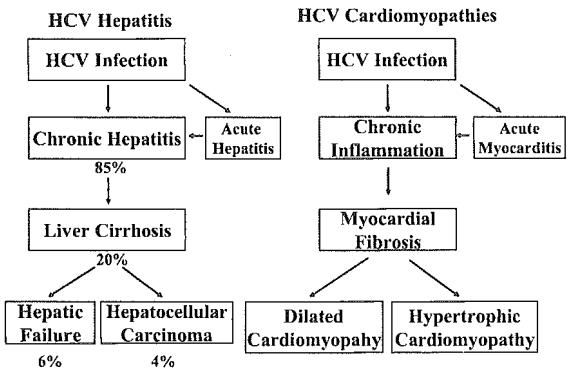

Figure 3. Comparison of the pathogenesis of HCV hepatitis and cardiomyopathies.

The pathogeneses of HCV hepatitis and cardiomyopathies are compared in Figure 3. In HCV liver disease, most patients develop chronic hepatitis and, years later, liver cirrhosis, hepatic failure, or hepatocellular carcinoma. In HCV heart disease, most patients develop chronic inflammation of the myocardium and, later, dilated cardiomyopathy attributable to necrosis and loss of myocytes. However, because myocytes do not replicate, proliferative stimuli induced by HCV infection may promote myocyte hypertrophy and hypertrophic cardiomyopathy.

We would like to propose a collaborative study of myocarditis/cardiomyopathies, based on a global network, to clarify the prevalence of cardiac involvement in HCV infection and to conduct a therapeutic trial.

Acknowledgments

I thank M. Ozone for preparing the manuscript.

References

1. Richardson P, McKenna W, Bristow M, Maisch B, Mautner B, O'Connell J, Olsen E, Thiene G, Goodwin J, Gyarfas I, Martin I, Nordet P. Report of the 1995 World Health Organization/International Society and Federation of Cardiology task force on the definition and classification of cardiomyopathies. *Circulation*. 1996;93:841–842.
2. Matsumori A, Kawai C. An animal model of congestive (dilated) cardiomyopathy: dilation and hypertrophy of the heart in the chronic stage in DBA/2 mice with myocarditis caused by encephalomyocarditis virus. *Circulation*. 1982;66:355–360.
3. Liu PP, Mason JW. Advances in the understanding of myocarditis. *Circulation*. 2001;104:1076–1082.
4. Matsumori A. Animal models: pathological findings and therapeutic considerations. In: Banatvala JE, ed. *Viral Infection of the Heart*. London, UK: E. Arnold; 1993:110–137.
5. Kawano H, Kawai S, Nishijo T, Shirai T, Inagaki Y, Okada R. An autopsy case of hypertrophic cardiomyopathy with pathological findings suggesting chronic myocarditis. *Jpn Heart J*. 1994;35:95–105.
6. Matsumori A, Matoba Y, and Sasayama S. Dilated cardiomyopathy associated with hepatitis C virus infection. *Circulation*. 1995;92:2519–2525.
7. Matsumori A, Matoba Y, Nishio R, Shioi T, Ono K, Sasayama S. Detection of hepatitis C virus RNA from the heart of patients with hypertrophic cardiomyopathy. *Biochem Biophys Res Commun*. 1996;222:678–682.
8. Okabe M, Fukuda K, Arakawa K, Kikuchi M. Chronic variant of myocarditis associated with hepatitis C virus infection. *Circulation*. 1997;96:22–24.
9. Matsumori A, Ohashi N, Nishio R, Kakio T, Hara M, Furukawa Y, Ono K, Shioi T, Sasayama S. Apical hypertrophic cardiomyopathy and hepatitis C virus infection. *Jpn Circ J*. 1999;63:433–438.
10. Takeda A, Sakata A, Takeda N. Detection of hepatitis C virus RNA in the hearts of patients with hepatogenic cardiomyopathy. *Mol Cell Biochem*. 1999;195:257–261.
11. Ooyake N, Kuzuo H, Hirano Y, Shimada T, Matsumori A. Myocardial injury induced by hepatitis C virus and interferon therapy [Abstract]. *J Jpn Soc Int Med*. 1999;88(suppl):241.
12. Sato Y, Takatsu Y, Yamada T, Kataoka K, Taniguchi R, Mimura R, Sasayama S, Matsumori A. Interferon treatment for dilated cardiomyopathy and striated myopathy associated with hepatitis C virus infection based on serial measurements of serum concentration of cardiac troponin T. *Jpn Circ J*. 2000;64:321–324.
13. Nakamura K, Matsumori A, Kusano KF, Banba K, Taniyama M, Nakamura Y, Morita H, Matsubara H, Yamanari H, Ohe T. Hepatitis C virus infection in a patient with dermatomyositis and left ventricular dysfunction. *Jpn Circ J*. 2000;64:617–618.

14. Matsumori A, Yutani C, Ikeda Y, Kawai S, and Sasayama S. Hepatitis C virus from the hearts of patients with myocarditis and cardiomyopathy. *Lab Invest.* 2000;80:1137–1142.
15. Matsumori A, Ohashi N, Ito H, Furukawa Y, Hasegawa K, Sasayama S, Naruse T, Inoko H, and co-investigators. Genes of the major histocompability complex class II influence the phenotype of cardiomyopathies associated with hepatitis C virus infection. In: Matsumori A, ed. *Cardiomyopathies and Heart Failure.* Boston, Mass: Kluwer Academic Publishers; 2003:515–521.
16. Omura T, Yoshiyama M, Hayashi T, Nishiguchi S, Kaito M, Horiike S, Fukuda K, Inamoto S, Kitaura Y, Nakamura Y, Teragaki M, Tokuhisa T, Iwao H, Takeuchi K, Yoshikawa J. Core protein of hepatitis C virus induces cardiomyopathy. *Circ Res.* 2005;96:148–150.
17. Tsutsumi T, Suzuki T, Moriya K, Yotsuyanagi H, Shintani Y, Fujie H, Matsuura Y, Kimura S, Koike K, Miyamura T. Alteration of intrahepatic cytokine expression a AP-1 activation in transgenic mice expressing hepatitis C virus core protein. *Virology.* 2002;304:415–424.
18. Eisen-Vandervelde AL, Waggoner SN, Yao ZQ, Cale EM, Hahn CS, Hahn YS. Hepatitis C virus core selectively suppresses interleukin-12 synthesis in human macrophages by interfering with AP-1 activation. *J Biol Chem.* 2004;279:43479–43486.
19. MacDonald A, Crowder K, Street A, McCormick C, Saksela K, Harris M. The hepatitis C virus non-structural NS5A protein inhibits activating protein-1 function by perturbing ras-ERK pathway signaling. *J Biol Chem.* 2003;278:17775–17784.
20. Erhardt A, Hassan M, Heintges T, Haussinger D. Hepatitis C virus core protein induces cell proliferation and activates ERK, JNK, and p38 MAP kinases together with the MAP kinase phosphatase MKP-1 in a HepG2 Tet-Off cell line. *Virology.* 2002;292:272–284.
21. Watashi K, Hijikata M, Marusawa H, Doi T, Shimotohno K. Cytoplasmic localization is important for transcription factor nuclear factor-kappa B activation by hepatitis C virus core protein through its amino terminal region. *Virology.* 2001;286:391–402.
22. Matsumori A, Furukawa Y, Hasegawa K, Sato Y, Nakagawa H, Morikawa Y, Miura K, Ohno Y, Tamakoshi A, Inaba Y, Sasayama S. Epidemiologic and clinical characteristics of cardiomyopathies in Japan: results from nationwide surveys. *Circ J.* 2002;66:323–336.
23. Matsumori A. Role of hepatitis C virus in myocarditis and cardiomyopathies. *J Geriatr Cardiol.* 2004;1:83–89.
24. Teragaki M, Nishiguchi S, Takeuchi K, Yoshiyama M, Akioka K, Yoshikawa J. Prevalence of hepatitis C virus infection among patients with hypertrophic cardiomyopathy. *Heart Vessels.* 2003;18:167–170.
25. Mason JW, O'Connell JB, Herskowits A, Rose NR, McManus BM, Billingham ME, Moon TE. A clinical trial of immunosuppressive therapy for myocarditis. The Myocarditis Treatment Investigators. *N Engl J Med.* 1995;333:269–275.
26. Alter MJ, Kruszon-Moran D, Nainan OV, McQuillan GM, Gao F, Moyer LA, Kaslow RA, Margolis HS. The prevalence of hepatitis C virus infection in the United States, 1988 through 1994. *N Engl J Med.* 1999; 341:556–562.
27. Matsumori A, Chapman NM, Tracy SM, Mason JW. Hepatitis C virus infection as a cause of myocarditis and heart failure. *Circulation.* 2004; 110(supp III):366.

KEY WORDS: hepatitis C virus ■ cardiomyopathy ■ myocarditis ■ heart failure ■ interferon

This un-edited manuscript has been accepted for publication in Biophysical Journal and is freely available on BioFast at http://www.biophysj.org. The final copyedited version of the paper may be found at http://www.biophysj.org.

An X-ray Diffraction Study on Mouse Cardiac Cross-Bridge Function in vivo : Effects of Adrenergic β-stimulation

Authors Ryuji Toh[#] Masakazu Shinohara,[#] Tomofumi Takaya, Tomoya Yamashita, Shigeru Masuda, Seinosuke Kawashima, Mitsuhiro Yokoyama, Naoto Yagi*
#These authors contributed equally to this article.

Affiliations Division of Cardiovascular and Respiratory Medicine, Department of Internal Medicine, Kobe University Graduate School of Medicine, Kobe 650-0017, Japan., *SPring-8/JASRI, Sayo, Hyogo 679-5198, Japan.

Corresponding author
N. Yagi
SPring-8/JASRI, Kouto, Sayo, Hyogo 679-5198, Japan.
Tel: +81-791-58-0908, Fax: +81-791-58-0830, Email: yagi@spring8.or.jp

Running title: X-ray diffraction of mouse heart in vivo

Keywords

x-ray diffraction, myosin cross-bridge, adrenergic β-stimulation

Abstract

In order to investigate how β-stimulation affects the contractility of cardiac muscle, x-ray diffraction from cardiac muscle in the left ventricular free wall of a mouse heart was recorded in vivo. This is the first x-ray diffraction study on a heart in a living body. After the R-wave in electrocardiograms, the ratio of the intensities of the equatorial (1,0) and (1,1) reflections decreased for about 50 msec from a diastolic value of 2.1 to a minimum of 0.8, and then recovered. The spacing of the (1,0) lattice planes increased for about 90 msec from a diastolic value of 37.2 nm to a maximum of 39.1 nm, and then returned to the diastolic level, corresponding to about 10% stretch of sarcomere. Stimulation of β-adrenergic receptor by dobutamine (20 μg/kg/min) accelerated both the decrease in the intensity ratio, which reached a smaller systolic value, and the increase in the lattice spacing. However, the intensity ratio and spacing at the end-diastole were unchanged. The recovery of the lattice spacing during relaxation was also accelerated. The mass transfer to the thin filaments at systole in a β-stimulated heart was close to the peak value in twitch of frog skeletal muscle at 4 °C, showing that the majority of cross-bridges have been recruited with few in reserve.

Introduction

Stimulation of cardiac β-adrenergic receptors has been known to enhance contractility of cardiac muscle through phosphorylation of various enzymes including troponin-I, C-protein and phospholamban (1-6). Although these effects have been extensively studied both physiologically and biochemically in isolated cardiac muscles and myocytes, they can be studied in a living body by only a limited number of methods. Lack of a molecular index that can be measured in vivo has made it difficult to study the mechanism of the β-stimulation. Since the overall influence of neurohumoral factors on functional properties of cardiac muscle can only be studied in vivo, it is important to develop a method to monitor contractility at the molecular level in a live animal. This is especially important when investigating the consequences of genetic alterations.

It is usually difficult to study murine, especially mouse, cardiac muscle in an isolated specimen under physiological conditions. Perfusion with oxygenated saline does not provide enough oxygen and a heart tends to be in a hypoxic condition at physiological heart rates. Although an x-ray diffraction study on an intact rat papillary muscle has an advantage that force and sarcomere length can be measured simultaneously, such experiments have been made at a heart rate lower than 1 Hz (7,8). Since the heart rate is an important factor in cardiac physiology, which affects calcium handling and contractile force, it is necessary to make these experiments at higher heart rates. This is especially the case if the increase in the contractile force with increased heart rate (staircase phenomenon) is due to higher number of cross-bridges associated with the thin filament during diastole (9).

X-ray diffraction has been used to study contractility of cardiac muscle. It is a non-invasive method which enables us to study myosin cross-bridge activity in striated muscles (10). Two pieces of information can be obtained: one is the intensity ratio of the (1,0) and (1,1) equatorial reflections from the hexagonal lattice of myofilaments, which can be used as an index of the number of myosin cross-bridges formed during contraction (mass transfer from the thick to the thin filament). This correlates well with tension development in cardiac muscle, especially during the early phase of contraction under an isometric condition (9). Theoretically, the intensity ratio might be affected by a conformational change of cross-bridges. However, experiments on skeletal muscle showed that a force-generating conformational change does not affect the ratio (11). Thus, the change in the ratio is mostly caused by a mass movement from the thick filaments to the thin filaments due to cross-bridge formation. The

other piece of available information is the (1,0) spacing of the lattice, which is equal to $\sqrt{3}/2$ of the distance between neighboring thick filaments. Since the volume of a cardiac cell remains approximately constant during a cardiac cycle (7), the lattice spacing can be used as an index of sarcomere length.

Recently, it was shown that diffraction patterns from a whole heart can be interpreted based on the orientation of muscle fibers in the heart (12), and a time-resolved x-ray diffraction study was made on a heart of a thoractomized rat (13). Here we applied this technique to a heart in a body of a living mouse to study physiological functions of myosin cross-bridges in vivo. Without thoractomizing, this is the first time the contractility in heart muscle was studied at a molecular level in a living body. Effects of β-stimulation by dobutamine was investigated.

Methods

Animal preparation

Eight-week old male mice (C57BL/6, purchased from CLEA Japan Inc., Tokyo, Japan) was anesthetized with isoflurane (0.25 - 0.5 %) and artificially ventilated (MiniVent™, Hugo Sachs Elektronik, March-Hugstetten, Germany; stroke volume 200 μl, 250 strokes/min). To avoid strong x-ray diffraction spots from skeletal muscles (see below), part of the breast muscles were surgically removed. The mouse was fixed vertically in the x-ray beam, which entered the thorax from the third intercostal space. In this configuration, the x-ray beam passed through the upper part of the left ventricle, whose motion during a heart beat is smaller than in the lower part. The electrocardiogram was recorded with three electrodes (Figure 1). Systemic blood pressure was measured by a computerized tail-cuff apparatus (MK-2000, Muromachi Kikai Co., Tokyo, Japan). The ventilator was stopped during an x-ray exposure (for about 2 sec) to avoid movement due to respiration. Dobutamine was infused from carotid artery with a rate of 20 μg/kg/min. The animal experiments were conducted in accordance with the guidelines of SPring-8 for care and welfare of experimental animals.

X-ray diffraction methods

X-ray diffraction experiments were conducted at BL40XU in the SPring-8 third generation synchrotron radiation facility (Harima, Hyogo, Japan) (14). The peak x-ray energy was adjusted to 15.0 keV. This high energy ensured sufficient

penetration of x-rays through a body of a mouse. The x-ray flux was adjusted by the front-end slits and aluminum absorbers to about 3×10^{12} photons/sec. The beam size was approximately 0.10 mm vertically, 0.25 mm horizontally at the specimen.

The x-ray detector was an x-ray image intensifier with a beryllium window (V5445P, Hamamatsu Photonics, Hamamatsu, Japan) (15) coupled by a tandem lens to a fast CCD camera (C4880-80-24A, Hamamatsu Photonics). The time resolution was 15 msec/frame. An x-ray shutter was opened for 1.1 sec and 70 successive frames were recorded. The specimen-to-detector distance was 3.2 m. The lattice spacing was calibrated with the third-order meridional reflection from the thick filament of frog skeletal muscle at 1/14.34 nm^{-1}. Both the electrocardiogram and the frame timing signal from the CCD camera were recorded with a data acquisition system with 1-msec sampling.

Experimental protocol

Since there are layers of skeletal muscles in the path of the x-ray beam, diffraction patterns from a mouse heart in vivo are always mixed with equatorial diffraction spots from skeletal muscles. With a mouse positioned vertically and an x-ray beam passing between the third and fourth ribs, usually two sets of spots were found in the directions of 10 o'clock and 4 o'clock, and 9 o'clock and 3 o'clock (Figure 2). The areas between these spots were free from reflections due to skeletal muscles. Initially, the x-ray beam was positioned in the left side of a mouse thorax (Figure 3, position A). Then, the mouse was moved across the beam horizontally so that its left ventricular free wall comes into the beam (Figure 3, position B). When the x-ray beam passed through the epicardium of the free wall, the equatorial reflections, which appear as spots (12), were observed in the directions similar to those of skeletal muscles. Thus, the epicardium surface plane seems to be approximately vertical in the mouse body. At this position, the movement of the heart due to beating shifted the heart in and out of the beam in every heart beat, making it impossible to observe the diffraction pattern continuously. When the mouse was moved further and the x-ray beam passed through the deeper layer of the free wall (Figure 3, position C), the equatorial diffraction pattern became arcs (12). At this stage, it was still difficult to observe the diffraction pattern continuously because the beam passed through different regions of the wall in diastole and systole. When the mouse was moved further in the beam (Figure 3, position D), the diffraction pattern appeared as a ring or a long arc with maximum intensity in the direction perpendicular to the diffraction from skeletal muscles (Figure 2). The diffraction pattern was continuously observed during a heart